Microb Ecol (1990) 19:269–278

MICROBIAL ECOLOGY

Differential Adhesion, Activity, and Carbohydrate : Protein Ratios of *Pseudomonas atlantica* Monocultures Attaching to Stainless Steel in a Linear Shear Gradient

M. W. Mittelman, D. E. Nivens, C. Low, and D. C. White

Institute for Applied Microbiology, University of Tennessee, Knoxville, Tennessee 37923, USA

Abstract. Biofilm formation on metallic surfaces in marine and freshwater environments often precedes corrosion and other biofouling conditions. Attachment is mediated by such environmental factors as the presence of surface conditioning films, fluid dynamics, bulk-phase nutrient levels, and surface chemistry. In this study, we utilized a Fowler Cell Adhesion Measurement Module to demonstrate that the changes in cellular concentration and composition of a monoculture of *Pseudomonas atlantica* biofilms on stainless steel were a function of the applied shear force. At shear forces in the range of 3–10 dynes cm^{-2} (1.0 liter min^{-1}), attachment as measured by acridine orange direct microscopic counts was greatest at the higher shear forces. ^{14}C-Acetate uptake activity on the stainless steel surfaces increased with shear stress. Acetate incorporation ranged from 1×10^{-5} to 19×10^{-5} μmol cm^{-2} between 0.15 and 30 dynes cm^{-2} for 30 min uptake periods. On a per cell basis, however, activity decreased with shear, indicating a shift in metabolism. Fourier transform infrared spectroscopy revealed that protein and carbohydrate concentrations also increased with the applied shear. Increased biofilm C:N ratios and total fatty acids were associated with the higher shear stresses. Neither radius of interaction nor biofilm age appeared to significantly influence the relationship between fluid shear and attachment and cellular composition of *P. atlantica* biofilms in the range of 1–10 dynes cm^{-2}.

Introduction

Bacteria possess a number of adaptive mechanisms enabling response to physicochemical factors defining their environment. One important mechanism is the ability of bacteria to adhere to surfaces in various environments. Zobell [25] proposed early on that solid surfaces serve to concentrate nutrients by adsorption. Venosa [22] and Costerton and Lashen [7], among others, have noted that sessile organisms are afforded protection from antagonistic agents such as lytic bacteria and biocidal agents. Bacterial biofilms play an important role in disease processes, degradation of industrial products and fluid-handling systems, wastewater treatment operations, and environmental ecosystems [5, 6, 18].

A number of theories relating environmental and physiological factors to bacterial adhesion processes have been proposed. Initial colonization and biofilm stability appear to be dependent on physicochemical factors such as interfacial surface energy [1, 21] hydrophobic interactions [16], and bulk phase substrate concentrations [4, 9, 12]. Young and Mitchell [24] showed that chemotaxis in marine systems could play a role in the initial colonization of motile bacteria. Mamur and Ruckenstein [11] demonstrated that gravitational forces significantly influenced the transport of cells to substrata in quiescent aqueous environments.

In addition to these physicochemical factors, fluid hydraulic parameters such as shear force and turbulence have also been shown to affect the adhesion process. Sly et al. [19] found that biofilm formation and manganese deposition rates in a potable water system were significantly increased at a higher water velocity. The deposition rate of *Streptococcus sanguis* on glass capillary tubes was shown by Rutter and Leach [17] to be a function of both nutrient loading and fluid velocity. Duddridge et al. [8] observed decreases in direct microscopic *Pseudomonas fluorescens* cell counts with increasing fluid shear in the range of 30–130 dynes cm^{-2}. However, relatively little is known about what effects shear forces have on the formation and nature of biofilms. While increased fluid velocity (shear) may overcome those electrostatic and covalent forces which result in "irreversible" adhesion, decreased substrate transport rates associated with low velocities could result in desorption of adhered cells.

In this study, the effects of fluid shear on the biomass constituents and metabolic activity of *P. atlantica* biofilms attaching to polished stainless steel surfaces are reported. Protein, carbohydrate and cell wall fatty acid content were measured as indicators of attached biomass. Incorporation of ^{14}C-1-acetate into membrane fatty acids was measured over a range of applied fluid shears. A radial-flow chamber [10] was utilized in these studies, allowing assays to be performed on the effects of multiple shear forces on single test coupons.

Materials and Methods

Test Organism. The marine bacterium, *P. atlantica* ATCC 19262, was used in all shear studies. The organism was maintained on three-quarter strength 2216 Marine Agar (Difco Laboratories, Detroit, MI) slants at 25°C. A minimal marine medium (MMB), described below, was used to develop inocula for the continuous culture system. The inoculum was obtained from "collars" which formed at the air/medium interface in 18–24 hour shake flask cultures. This culture isolation process was employed to select for adherent variants within the monoculture.

Continuous Culture Conditions. A Virtis 1 liter OmniCulture system with a 600 ml working volume (Gardiner, NY) was used to maintain cultures at constant conditions of temperature (25°C), aeration (1 liter/min^{-1}), agitation (100 rpm), and dilution rate (d = 0.1 $hour^{-1}$). All reagents utilized in this study were of analytical reagent grade, unless otherwise specified. The culture and shake flask medium consisted of the following ingredients in g $liter^{-1}$ deionized water: artificial sea salts, 30; galactose, 0.5; NH_4Cl, 0.1; Tris HCl/base, 100 mM; $MgCl_2 \cdot 6H_2O$, 0.4; $K_2HPO_4 \cdot 3H_2O$, 0.4; $FeCl_3$, 4 mM; and 1 ml Wolfe's complex vitamin mixture. The galactose, $FeCl_3$, and vitamin mixture were filter-sterilized and added separately to the autoclaved and cooled medium. The complete medium had a pH of 7.5 and buffering capacity was sufficient to maintain this pH throughout the test period.

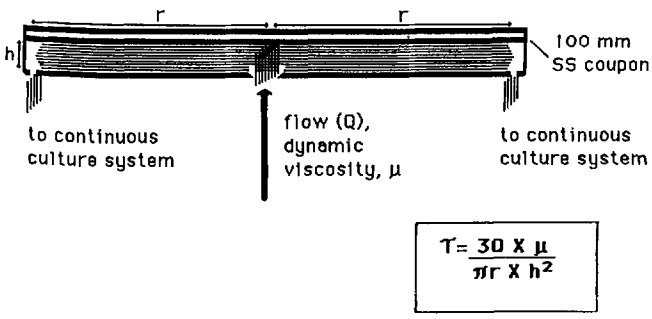

Fig. 1. Vertical section of cell adhesion measurement module showing direction of flow and shear generation. Shear force is inversely proportional to radius, with the greatest shear forces generated near the entry zone. The parallel plate separation distance, h, was maintained at 1 mm.

Cell Adhesion Measurement Module (CAMM)

A radial-flow cell described by Fowler and McKay [10] was employed to facilitate development of a continuous shear gradient across 100 mm diameter, 600-grit finished 316 stainless steel coupons (Fig. 1). Culture medium and suspended bacterial cells contacted the center of the test coupon; shear, τ, was generated radially, in inverse proportion to the radius. Medium and cells exited the CAMM at the outer edge of the coupon, approximately 50 mm from the entry zone. Flow rates through the system were maintained such that a Reynolds number of <2,000, indicating laminar flow, was obtained. Flow rates were maintained at a constant value in the range of 60–1,000 ml min^{-1}. Several flow rates in this range were employed to generate data in the experiments described herein. Pulseless pumps and silicone tubing were used throughout the system.

Test Procedure. Following steam-sterilization, the test system was aseptically assembled and filled with sterile culture medium. Following a 24 hour sterility test, ca. 1×10^9 adherent cells from a shake flask were inoculated into the continuous culture vessel. Dissolved oxygen (DO) levels in the bulk phase were monitored thoughout the experiment using a YSI model 50 DO meter/probe (Yellow Springs Instruments, Yellow Springs, OH); DO levels varied from saturation (ca. 8.2 mg $liter^{-1}$) at T = 0 hours to 5.75 mg $liter^{-1}$ at T = 120 hours.

Following the recirculation period, test coupons were aseptically removed from the CAMM and either analyzed immediately (as with acridine orange counts and activity measurements) or frozen at −50°C, lyophilized, and stored in a vacuum desiccator until ready for further study.

Analytical Procedures. Coupons for direct observation and microscopic cell counts were stained for 5 min in 0.1 mg ml^{-1} acridine orange (Sigma, St. Louis, MO) in 100 mM phosphate buffer, pH 7.5, containing 2% (v/v) glutaraldehyde. Coupons were observed directly under epifluorescent illumination. Coupons were also quantitatively extracted for microscopic direct cell counts using 1.2 cm diameter glass o-ring extractors (Kontes Glass, Vineland, NJ). Following addition of 0.6 ml volumes of the minimal medium to the extractors, the surfaces were sonicated to remove adherent cells using three 3-sec pulses at 20% power (Heat Systems sonicator, Plainview, NY). Preliminary experiments (data not shown) demonstrated that >95% of the adherent cells and associated biomass material could be removed by this extraction procedure. The sonicated suspensions were fixed in 2% (v/v) glutaraldehyde, then filtered through 0.2 μm polycarbonate filters (Nuclepore Corp., Pleasanton, CA). Dried filters were fixed onto glass microscope slides with immersion oil, then examined under epifluorescence illumination.

Lyophilized and desiccated coupons were analyzed by diffuse reflectance IR spectroscopy (DRIFT) on a Nicolet model 60 SX Fourier transforming infrared spectrometer (Nicolet Instruments, Madison, WI) equipped with a standard Globar source, a KBR beam splitter, a narrow band liquid nitrogen-cooled HgCdTe detector (Nicolet Instruments), and an Analect Instruments (Utica, NY) DRIFT device. The data were collected as single-sided interferograms with a resolution of 8 cm^{-1} at a mirror retardation velocity of 1.570 cm sec^{-1}. Coupons were scanned at multiple radii; four measurements per radius were taken at 90° angles. Absorbances were measured at reciprocal

wavelengths ranging from 800 to 2,000 cm^{-1}, with 250 scans per measurement. Interferograms were Fourier processed using phase correction and a Happ-Genzel appodization function. A ratio of biofilm absorbances against those obtained from clean stainless steel coupons were determined, baseline corrected, and water vapor subtractions were performed when necessary. The final spectra were converted to Kubelka-Munk units and were smoothed using a five point least squares quadratic smoothing algorithm [13]. Coupon manipulations were carried out in a dry nitrogen atmosphere to limit interferences associated with water vapor.

Coupons were quantitatively extracted for protein and total lipids via sonication as described above. Protein was measured using a sodium dodecyl sulfate-modified Lowry procedure [14] with a bovine serum albumin standard. Total lipids were extracted using the glass o-ring extractors equipped with Kalrez o-rings. Following the recirculation period, the coupon was immediately removed from the CAMM, o-ring extractors were clamped in place, and 0.6 ml chloroform-methanol-water reagent [Bligh-Dyer cocktail; 2] was added to the surface of each extraction area. Following a 2 hour extraction period, the 0.6 ml aliquots were decanted to 13 × 100 mm test tubes. The coupon surfaces were rinsed with two 0.6 ml aliquots of the Bligh-Dyer cocktail. The contents of the 13 × 100 mm test tubes were then transferred to 30 ml separatory funnels; after addition of chloroform and water to effect phase separation, the mixture was allowed to extract for 24 hours at room temperature. The organic phase was then subjected to a mild alkaline methanolysis [15, 20]. Phospholipids were analyzed using a modification of the method of White et al. [23]. Fatty acid methyl esters were quantitated directly using a Hewlett-Packard model 5880 gas chromatograph equipped with a capillary column as described by Ringelberg et al. [15]. Confirmation of fatty acid identification was made on a Hewlett-Packard model 5996A GC/MS.

Pulse labeling of the biofilm coupons was performed in situ by recirculating 1-^{14}C-acetate through the CAMM at the in situ flow rate. A 100 ml volume of MMB containing 0.5 μCi ml^{-1} sodium acetate with a specific activity of 55.0 mCi $mmol^{-1}$ (New England Nuclear, Boston, MA) was recirculated for 30 min. Following the recirculation period, the coupon was immediately removed from the CAMM. No rinsing of the coupons was performed prior to the extraction. Total fatty acids were extracted from various areas on the labeled coupon surface as described above. The organic phase from the Bligh-Dyer extraction (which contained the labeled lipids) was transferred to 7 ml scintillation vials, made basic by addition of 0.1 M KOH, then dried under a gentle nitrogen stream. Following addition of 4.0 ml scintillation cocktail (Econolume, ICN, Irvine, CA), the samples were counted on an LKB model 1212 (Gaithersburg, MD) liquid scintillation counter. The counts were quench corrected using a series of external quench standards (Packard, Downers Grove, IL).

Results

Influence of Shear on Biomass Development

Figure 2 illustrates the spectra of a 48 hour *P. atlantica* biofilm at several fluid shear regimes. The peaks appearing at 1,630 cm^{-1} and 1,550 cm^{-1} correspond to the amide I and amide II regions, respectively, of proteins. The region from 1,000 to 1,200 cm^{-1} contains peaks corresponding to the C-O stretch of carbohydrates. A phosphate band appears at 1,240 cm^{-1}. A significant positive correlation ($P < 0.05$) was observed between fluid shear and the absorbances of these distinctive bands. The absorbance values tended to increase with applied shear up to a critical value which defined the limit of attachment. The transitional area, where absorbance values drop precipitously, typically appeared within 5 to 10 mm of the central impact area.

Direct epifluorescent microscopic observation of coupon surfaces revealed the presence of greater numbers of bacteria associated with the higher shear

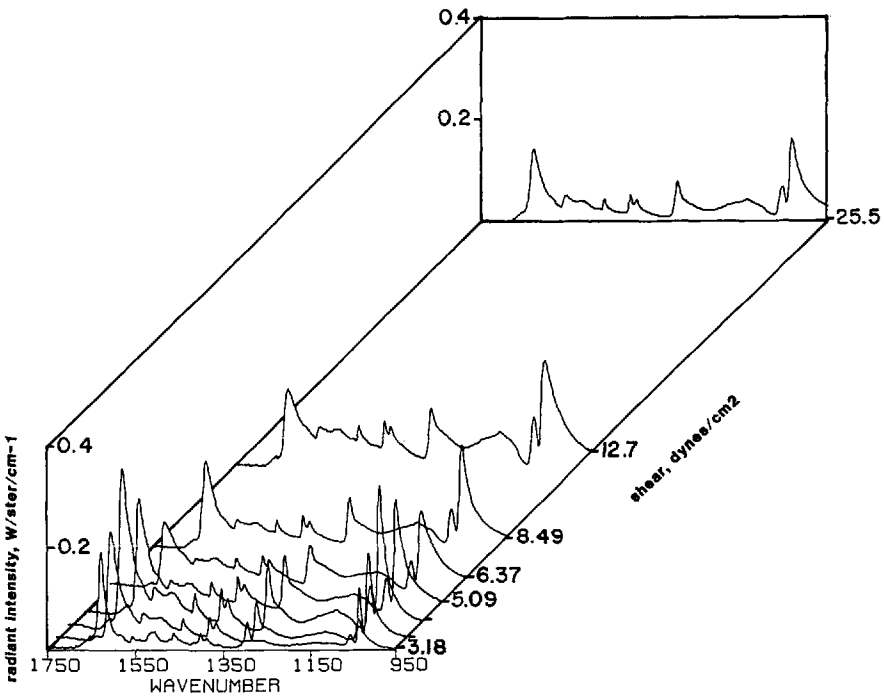

Fig. 2. FTIR spectra of *P. atlantica* exposed to varying shear stresses. Amide I and II absorbance values are considered indicative of proteinaceous biomass; the CHO absorbances at 1,100–1,130 cm^{-1} are representative of the C-O stretch associated with carbohydrate groups (e.g., polysaccharides).

areas of the coupon (Table 1). The cells attached to the higher shear areas appeared to be smaller in size than those associated with the low shear areas. Total cell counts were significantly affected by shear in the range of 3 to 13 dynes cm^{-2}. Total bacteria counts ranged from 1.5×10^5 at 1.1 dynes cm^{-2} to 5.7×10^7 cells cm^{-2} at 13 dynes cm^{-2}. Total protein (Fig. 3) and phospholipid fatty acid biomass parameters (Table 2) were significantly influenced by shear effects in the range of 0.2 to 31 and 1 to 8 dynes cm^{-2}, respectively.

Compositional Changes with Shear

An increase in the ratio of carbohydrate to amide II IR absorbance was related to shear in the range of 0.2 to 29 dynes cm^{-2} (Fig. 3). A similar relationship was apparent between the carbohydrate : amide I ratio and shear (data not shown). The results of the DRIFT/FTIR analysis indicate that biomass as carbohydrate and protein on a per unit area basis increased with increasing fluid shear. The ratio of saturated : unsaturated fatty acids, a measure of membrane fluidity, was not significantly affected by shear. The ratios varied from 0.75 to 0.85 between 1 and 8 dynes cm^{-2} (Table 2).

Table 1. Direct counts and activity of *P. atlantica* on coupon surfaces exposed to fluid shear

Mid-range shear[a] dynes cm^{-2}	Mean number of attached bacteria[b] cells cm^{-2} (±1 SD) × 10^6	Acetate incorporation μmol/cell^{-1}[c] (× 10^{-13}) (±1 SD)
1.06	0.15 (0.074)	nt
2.39	0.99 (0.49)	nt
3.62	1.4 (0.79)	17.7 (6.4)
4.97	7.8 (5.5)	2.48 (1.68)
7.96	41.0 (8.8)	0.36 (0.25)
13.0	56.8 (18.6)	nt

[a] Values for shear at the center of 1.2 cm diameter extraction areas are reported
[b] Average of counts taken from four different extraction areas per shear value; a one-way analysis of variance was performed: $P < 0.01$
[c] Average of four 30-min uptake measurements taken at each shear value; a one-way analysis of variance was performed: $P < 0.01$

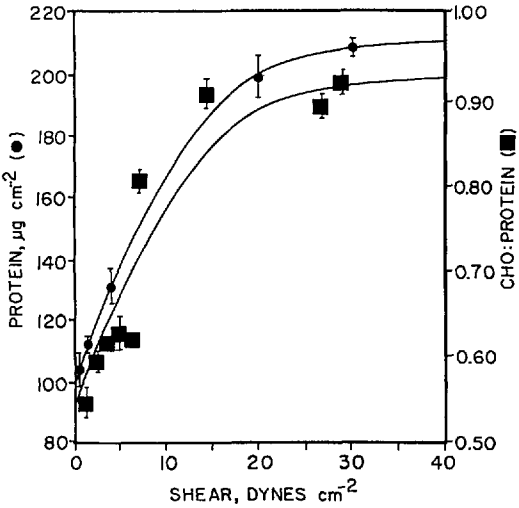

Fig. 3. Ratio of carbohydrate (1,130 cm^{-1}) to amide II (■) (1,550 cm^{-1}) IR absorbances for *P. atlantica* biofilms exposed to varying shear stresses. Total protein (●) vs shear; four replicates per shear, error bars represent ±1 SD.

Metabolic Activity

The amount of ^{14}C-1-acetate incorporation into lipids increased linearly with fluid shear. Thirty-minute uptake values ranged from 1×10^{-5} to 19×10^{-5} μmol cm^{-2} between 0.15 and 30 dynes cm^{-2}. Normalizing the uptake data with respect to cell counts, however, revealed a statistically significant decline in uptake with increased shear in the range of 1–10 dynes cm^{-2}. A 2.2-fold increase in shear resulted in a 49-fold decrease in acetate incorporation during the 30-minute uptake experiments (Table 1).

Table 2. Total fatty acid biomass and saturated : unsaturated fatty acid ratios vs fluid shear

Mid-range shear[a] dynes cm^{-2}	Total phospholipid fatty acids[b] pmol cm^{-2} (±1 SD)	Saturated : unsaturated fatty acids (±1 SD)
1.09	442.0 (143.5)	0.65 (0.09)
3.62	764.4 (138.5)	0.72 (0.07)
4.97	786.1 (84.3)	0.76 (0.07)
7.96	1,244.8 (289.9)	0.74 (0.01)

[a] Values for shear at the center of 1.2 cm diameter extraction areas are reported

[b] Average of measurements taken from four different extraction areas per shear value; a one-way analysis of variance was performed: $P < 0.01$ for total lipids; $P > 0.1$ for saturated : unsaturated fatty acids

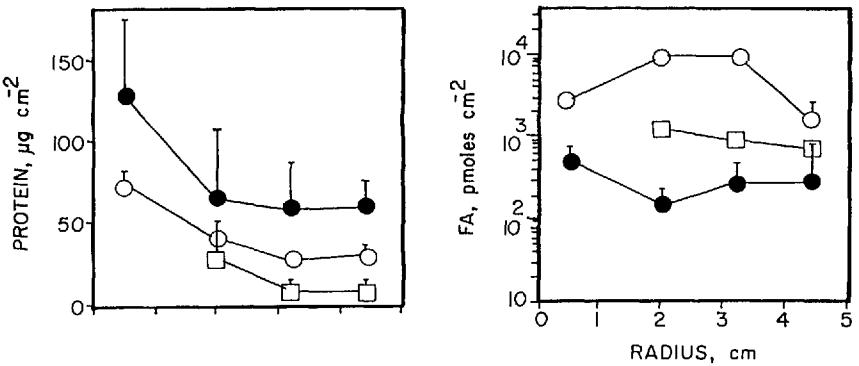

Fig. 4. Protein and total fatty acids as biomass vs coupon radius. Four replicates from each of three biofilm development periods were obtained per radius; error bars represent ±1 SD. 48 h (□), 72 h (●), 120 h (○).

Effect of Radius and Time on Biomass

There was little effect of radius on protein or fatty acid biomass parameters (Figs. 4a and b). Tests of significance using first and second order regression coefficients did not reveal a significant effect of radius on bacterial adhesion or acetate incorporation into phospholipid fatty acids in 1–10 dynes cm^{-2} ($P > 0.10$; data not shown). The data indicated that location on the coupons did not influence cell density and that shear was the major biomass determinant.

The effect of biofilm age on biomass parameters under varying shear regimes was extremely variable within and among different time periods (data not shown). A statistically significant effect of biofilm age could not be demonstrated for any of the measured biomass development parameters ($P > 0.10$).

Discussion

In most environments, bacterial adhesion processes proceed under some hydraulic influences. Bacterial adhesion to surfaces in these environments is de-

pendent upon a balance between attractive and repulsive physicochemical forces. The results of this study demonstrated that mechanical factors such as fluid shear can potentiate bacterial colonization processes.

One explanation for the observed increase in cell counts with fluid shear could be an interaction between radius and bacterial attachment, that is, a recruitment phenomenon influenced by the frequency of cell-substratum contact and/or substrate transport. If this were the case, a relationship between attachment, biomass formation, and activity and radius should have been apparent. Under the experimental conditions imposed during this study, it is doubtful that recruitment played as significant a role as fluid shear in influencing bacterial attachment to stainless steel.

If bacteria are viewed as small particles lacking any purposive behavior (e.g., chemotaxis or polymer production), theoretical considerations dictate that their rate of deposition should increase with fluid velocity. Bowen and Epstein [3] showed that the local particle deposition rate in a parallel plate channel may be described by

$$J_D = DC_o \times \frac{(2/9\gamma)^{1/3}}{b\lambda(4/3) + (1/K)(2/9\gamma)^{1/3}}$$

where $\gamma = 2Dx/3V_m b^2$ is the dimensionless longitudinal distance from the inlet, $D = kT/6\pi\eta\alpha$ is the Stokes-Einstein diffusion coefficient, C_o is the particle concentration at the inlet, b is one-half the channel thickness, x the radius from the inlet, V_m the mean velocity of the fluid, k the Boltzmann constant, T the fluid temperature, η the viscosity of the fluid, α the average particle radius, K the surface reaction rate constant, and λ a mathematical function. The results of this study agree with these theoretical considerations; namely, that attachment is increased at higher flow rates up to a critical point. Beyond this critical flow (shear) the adhesive forces associated with bacterial substratum interactions are overcome by the "repulsive" forces of fluid shear.

When Rutter and Leech [17] studied the deposition of *Streptococcus sanguis* onto glass capillary tubes, they found that deposition was enhanced at higher fluid velocities when the bacteria were grown at a relatively low dilution rate (0.04 hour^{-1}). However, at higher dilution rates (>0.2 hour^{-1}), adhesion was decreased. They attributed this deviation from theory to "polymer bridging." Duddridge et al. [8] have reported that increased surface shear resulted in decreased attachment of *P. fluorescens* to stainless steel. However, their adhesion assays were conducted at higher fluid shear values, 60–1,100 dynes cm^{-2}. Observations of biofilms exposed to relatively high shear stresses indicate that the ability of *P. atlantica* to remain attached to polished stainless steel is greatly reduced beyond a fluid shear of approximately 120 dynes cm^{-2}.

The increase in carbohydrate : protein ratios with shear as measured by FTIR spectroscopy suggests that bacteria able to adhere at high shear force gradients show a shift in chemical structure. Previous work by Nichols et al. [13] showed that FTIR spectra of *P. atlantica* biofilms could be used to infer nutritional status. Here we show a change related to the shear environment. Perhaps cells which are initially adhered to the coupon surface stabilize the adhesion process via production of additional extracellular polymeric substances (EPS). If the

1,130 cm^{-1} band is indicative of EPS carbohydrate biomass, this would suggest that shear force induces the synthesis of EPS. Since the total Lowry protein and total cell count also increased with shear, the carbohydrate : protein ratio may be an indicator of adhesion stability in *P. atlantica* grown in a defined environment.

The observation that per cell lipid synthetic activity declined with increased shear could be an indication of shear induced stress on the organisms. Alternatively, a shift in biosynthesis from membrane lipids to extracellular adhesive moieties could also be envisioned. The increased per unit area metabolic activity seen with higher shear values correlates well with the observed biomass increases. These findings suggest that microbially influenced surface perturbations may be affected by hydraulic factors.

The methods described in this work provide a powerful tool for assessing the effects of environmental and cultural variables on biofilm development parameters under well-defined hydraulic conditions. These methods make possible studies of complex interactions among consortial members of sessile bacteria present in biofilms. We are now utilizing these techniques to explore the nature of bacterial succession under environmental conditions designed to approximate those of in situ aquatic environments.

Acknowledgments. This work was supported in part by a grant from the U.S. Navy Office of Naval Research, contract number N00014-87-K-0012. The helpful comments of Drs. T. J. Phelps and J. B. Guckert are acknowledged.

References

1. Absolom DR, Lamberti FV, Policova Z, Zingg W, van Oss C, Neumann AW (1983) Surface thermodynamics of bacterial adhesion. Appl Environ Microbiol 46:90–97
2. Bligh EG, Dyer EJ (1959) A rapid method of total lipid extraction and purification. Can J Biochem Physiol 37:911–917
3. Bowen BD, Epstein N (1979) Fine particle deposition in smooth parallel-plate channels. J Coll Inter Sci 72:81–97
4. Brown CM, Ellwood DC, Hunter JR (1977) Growth of bacteria at surfaces: Influence of nutrient limitation. FEMS Microb Lett 1:163–166
5. Characklis WG, Cooksey KE (1983) Biofilms and microbial fouling. Adv Appl Microbiol 29: 93–138
6. Costerton JW, Cheng K-J (1985) Phenomena of bacterial adhesion. In: Savage DC, Fletcher M (eds) Bacterial adhesion: Mechanisms and physiological significance. Plenum Press, New York, pp 3–43
7. Costerton JW, Lashen ES (1984) Influence of biofilm on efficacy of biocides on corrosion-causing bacteria. Materials Performance 23(2):13–17
8. Duddridge JE, Kent CA, Laws JF (1982) Effect of surface shear stress on the attachment of *Pseudomonas fluorescens* to stainless steel under defined flow conditions. Biotech Bioeng 24: 153–164
9. Fletcher M (1988) Attachment of *Pseudomonas fluorescens* to glass and influence of electrolytes on bacterium-substratum separation distance. J Bacteriol 170:2027–2030
10. Fowler HW, McKay AJ (1980) The measurement of microbial adhesion. In: Berkeley RCW, Lynch JM, Melling J, Rutter PR, Vincent B (eds) Microbial adhesion to surfaces. Harwood, Chichester, pp 143–161
11. Marmur A, Ruckenstein E (1986) Gravity and cell adhesion. J Coll Int Sci 114:261–266

12. Marshall KC (1988) Adhesion and growth of bacteria at surfaces in oligotrophic environments. Can J Microbiol 34:503–506
13. Nichols PD, Henson JM, Guckert JB, Nivens DE, White DC (1985) Fourier transform-infrared spectroscopic methods for microbial ecology: Analysis of bacteria, bacteria-polymer mixtures and biofilms. J Microbiol Meth 4:79–94
14. Peterson GL (1977) A simplification of the protein assay of Lowry which is more generally applicable. Anal Biochem 83:346–351
15. Ringelberg DH, Davis JD, Smith GA, Pfiffner SM, Yates P, Kampbell DH, Reed HW, Stocksdale TT, White DC (1988) Validation of signature phospholipid fatty acid biomarkers for alkane-utilizing bacteria in soils and subsurface aquifer materials. FEMS Microb Ecol 62: 39–50
16. Rosenberg M, Kjelleberg S (1986) Hydrophobic interactions: Role in bacterial adhesion. In: Marshall KC (ed) Advances in microbial ecology, vol 9. Plenum Press, New York, pp 353–393
17. Rutter P, Leech R (1980) The deposition of *Streptococcus sanguis* NCTC 7868 from a flowing suspension. J Gen Microbiol 120:301–307
18. Savage DC (1980) Adherence of normal flora to mucosal surfaces. In: Beachey EH (ed) Bacterial adherence, receptors and recognition, vol 6. Chapman and Hill, London, pp 33–59
19. Sly LI, Hodgkinson MC, Arunpairojana V (1988) Effect of water velocity on the early development of manganese-depositing biofilm in a drinking-water distribution system. FEMS Microb Ecol 53:175–186
20. Tunlid A, Ringelberg D, Low C, Phelps TJ, White DC (1989) Analysis of phospholipid fatty acids from bacteria at picomolar sensitivities from bacteria in environmental samples. J Microbiol Meth 10:139–153
21. van Loosdrecht MCM, Lyklema J, Norde W, Zehnder AJB (1989) Bacterial adhesion: A physiochemical approach. Microb Ecol 17:1–15
22. Venosa AD (1975) Lysis of *S. natans* swarm cells by *Bdellovibrio bacteriovirus*. Appl Microbiol 29:702–705
23. White DC, Davis WM, Nickels JS, King JD, Bobbie RJ (1979) Determination of the sedimentary microbiological biomass by extractable lipid phosphate. Oecologia 40:51–62
24. Young LY, Mitchell R (1972) The role of chemotactic response to primary microbial film formation. In: Acker RF (ed) Proc Third Int Congr Mar Corrosion Fouling. Northwestern Univ Press, Evanston, IL, pp 617–624
25. Zobell CE (1943) The effect of solid surfaces on bacterial activity. J Bacteriol 46:39–56.